

## On the structure of transient atmospheric waves. Part I

A. WIIN-NIELSEN

*Department of Atmospheric, Oceanic and Space Science, University of Michigan*

(Manuscript received April 27, 1988, accepted in final form August 2, 1988)

### RESUMEN

Se investiga la estructura de las ondas baroclínicas en una corriente zonal. Usando un modelo cuasi-nodivergente de dos capas, es posible derivar dos ecuaciones no lineales que describen los cambios con respecto al tiempo de la razón de las amplitudes y la diferencia del ángulo de fase entre la onda promediada verticalmente y la onda térmica. Se obtienen todos los estados estacionarios y sus propiedades de estabilidad lineal.

Los resultados muestran que hay un estado estacionario estable que tiene una onda con inclinación hacia el oeste que aumenta su amplitud con la altura, éste corresponde al estado asintótico de la onda baroclínica amplificada. Otro estado estacionario con la pendiente opuesta es inestable. Se encuentran cuatro estados estacionarios para cizallamientos del viento suficientemente pequeños, que son estables, pero de naturaleza oscilatoria, y que son o verticales o con una inclinación igual a la mitad de la longitud de onda.

### ABSTRACT

The structure of baroclinic waves on a zonal current is investigated. Using a two level, quasi-nondivergent model it is possible to derive two nonlinear equations describing the changes in time of the ratio of the amplitudes and the phase angle difference between the vertically averaged wave and the thermal wave. All steady states and their linear stability properties are found.

It turns out that one stable steady state describes a westward sloping wave increasing in amplitude with height. This state corresponds to the asymptotic state of the amplifying baroclinic wave. Another steady state with the opposite slope is unstable. Four additional steady states are found for sufficiently small windshears. They are stable, but of an oscillatory nature, and are either vertical or sloping half a wave length.

### Introduction

The observed structure of synoptic scale waves has been described in detail in numerous studies. Palmén and Newton (1969) give a detailed description of the properties of these waves, and they stress the westward slope with height of the waves. The slope can be seen by following the ridge and trough lines in vertical, zonal cross-sections. A westward tilt of the geopotential waves is consistent with a lag of the temperature field behind the geopotential field on tropospheric isobaric surfaces.

It is generally recognized that the observed waves exist due to the baroclinic instability of the zonal currents in the atmosphere. According to the results from studies by Charney (1947) and many others using various models, it is established that the atmosphere is almost always baroclinically unstable. From the results of the stability studies, it is possible to show that the unstable steady state results in baroclinic waves which slope westward with height provided the zonal current increases with height as shown by Ogura (1957) using a two-level model, but the problem is, of course, that the perturbation studies deal with infinitesimal disturbances while the atmosphere contains finite amplitude disturbances.

It may therefore be instructive to consider the problem in a different way. To keep the treatment as simple as possible, we shall adopt a two-level, quasi-nondivergent model and finite amplitude waves of a particularly simple form. Heating and dissipation will also be neglected for simplicity. In view of these assumptions, we shall be dealing with free waves, and we cannot expect to obtain absolute, but only relative values of the amplitudes. We shall, as a matter of fact, be able to derive equations for the relative amplitude and its development in time and for the phase-difference between the geopotential and thermal fields.

No analytic solution is available to these nonlinear equations. It is, however, possible to find all steady state solutions as a function of the wave length and the thermal wind. A following investigation of the stability of the steady states will show that one stable steady state will represent a wave which slopes westward with height. Other stable states exist for sufficiently small values of the wind shear and/or sufficiently small wave lengths, but these waves have supposedly minor importance because they are outside the region of baroclinic instability. In any case, these waves, as we shall see, have no slope in the vertical direction because the temperature field is either in phase with the geopotential field or lags this field by a phase angle corresponding to half a wave length.

The present study is a continuation of similar studies by Ogura (1957), Thompson (1959) and the author (1961). The present approach is different because it does not rely on the results of baroclinic instability studies, but on equations which describes the structure of the wave directly.

## 2. The model

As mentioned in the introduction, we use the **quasi-geostrophic** two-level model in this study. The model is described in many places in the literature (e.g., Wiin-Nielsen, 1973), and it will suffice to give the equations. They are:

$$\begin{aligned} \frac{\partial \xi_*}{\partial t} + \mathbf{V}_* \cdot \nabla \xi_* + \mathbf{V}_T \cdot \nabla \xi_T + \beta v_* &= 0 \\ \frac{\partial (\xi_T - q^2 \psi_T)}{\partial t} + \mathbf{V}_* \cdot \nabla (\xi_T - q^2 \psi_T) + \mathbf{V}_T \cdot \nabla \xi_* + \beta v_T &= 0 \end{aligned} \quad (2.1)$$

in which  $\xi = \nabla^2 \psi$  is the vorticity,  $\psi$  the stream function,  $\mathbf{V} = \mathbf{k} \times \nabla \psi$ , the horizontal, nondivergent wind,  $\beta = df/dy$ , where  $f$  is the Coriolis' parameter,  $q^2 = 2f_0^2/\sigma P^2$ , where  $\sigma = \alpha \partial \ln \theta / \partial p$  is the stability measure,  $\Theta$  the potential temperature,  $\alpha$  the specific volume,  $p$  pressure and  $P = 50$  cb. The reference levels for the model are 25 cb (subscript 1) and 75 cb (subscript 3). The subscripts \* and T are defined by

$$(*) = \frac{1}{2}[( )_1 + ( )_3]; \quad ( )_T = \frac{1}{2}[( )_1 - ( )_2] \quad (2.2)$$

The zonal flow will be characterized by the two constant velocities  $U_*$  and  $U_T$ . On the zonal flow we superimpose waves of a single wave number, i.e., we specify the following stream functions:

$$\begin{aligned} \psi_*(x, y, t) &= -U_* y + A(t) \cos kx + B(t) \sin kx \\ \psi_T(x, y, t) &= -U_T y + C(t) \cos kx + D(t) \sin kx \end{aligned} \quad (2.3)$$

The expressions (2.3) are substituted in (2.1) resulting in four equations as follows:

$$\begin{aligned}\frac{dA}{dt} &= -k(U_* - C_R)B - kU_T D; & C_R &= \frac{\beta}{k^2} \\ \frac{dB}{dt} &= k(U_* - C_R)A + kU_T C \\ \frac{dC}{dt} &= -k\left(U_* - \frac{C_R}{1 + q^2/k^2}\right)D - \frac{1 - q^2/k^2}{1 + q^2/k^2}kU_T B \\ \frac{dD}{dt} &= k\left(U_* - \frac{C_R}{1 + q^2/k^2}\right)C + \frac{1 - q^2/k^2}{1 + q^2/k^2}kU_T A\end{aligned}\quad (2.4)$$

It will be advantageous to introduce an amplitude and a phase angle for the waves in the mean field and the thermal field, say:

$$A = R_* \cos \theta_*, \quad B = R_* \sin \theta_*, \quad C = R_T \cos \theta_T, \quad D = R_T \sin \theta_T \quad (2.5)$$

Substitution of (2.5) in (2.4) yields the following equations:

$$\begin{aligned}\frac{dR_*}{dt} &= kU_T R_T \sin(\theta_* - \theta_T) \\ R_* \frac{d\theta_*}{dt} &= k(U_* - C_R)R_* + kU_T R_T \cos(\theta_* - \theta_T) \\ \frac{dR_T}{dt} &= -\frac{1 - q^2/k^2}{1 + q^2/K^2}kU_T R_* \sin(\theta_* - \theta_T) \\ R_T \frac{d\theta_T}{dt} &= k\left(U_* - \frac{C_R}{1 + q^2/k^2}\right)R_T + \frac{1 - q^2/k^2}{1 + q^2/k^2}kU_T R_* \cos(\theta_* - \theta_T)\end{aligned}\quad (2.6)$$

We may consider (2.6) as a predictive system, but we are not at the moment interested in the absolute position of the wave as specified by  $\theta_*$  and  $\theta_T$ , but rather in the ultimate structure of the wave. The important quantity is, therefore,  $\varphi = \theta_* - \theta_T$ . Subtracting the fourth equation in (2.6) from the second we find:

$$\frac{d\varphi}{dt} = -KC_R \frac{q^2/k^2}{1 + q^2/k^2} + kU_T \left(r - \frac{1 - q^2/k^2}{1 + q^2/k^2} \frac{1}{r}\right) \cos \varphi \quad (2.7)$$

in which  $r$  is defined by:

$$r = \frac{R_T}{R_*} \quad (2.8)$$

An equation for the rate of change of  $r$  may be obtained by noting that:

$$\frac{dr}{dt} = \frac{1}{R_*^2} \left( R_* \frac{dR_T}{dt} - R_T \frac{dR_*}{dt} \right). \quad (2.9)$$

Using (2.6) we then obtain:

$$\frac{dr}{dt} = -kU_T \left( \frac{1 - q^2/k^2}{1 + q^2/k^2} + r^2 \right) \sin\varphi \quad (2.10)$$

The nonlinear system (2.7) and (2.10) is the basic system for the remaining part of the study. It may be solved numerically, but we shall use the strategy of finding all steady states of the system and thereafter discuss the stability of them.

### 3. The steady states

In finding the steady states of (2.7) and (2.10), we note that  $r$  by definition is a positive quantity. From (2.10) it is then seen that the parenthesis on the right hand side cannot be zero when  $k > q$ . In this case we find from (2.10) that a steady state requires that  $\varphi = 0$  or  $\pi$ , corresponding to  $\cos\varphi = 1$  or  $\cos\varphi = -1$ , respectively. By using these values in (2.7), we find the following steady states:

$$k > q, \quad \varphi_s = 0$$

$$r_s = \frac{1}{2} \left[ \frac{C_R}{U_T} \frac{q^2}{q^2 + k^2} \pm D^{1/2} \right]; \quad D = \left[ \left( \frac{C_R}{U_T} \frac{q^2}{q^2 + k^2} \right)^2 + 4 \frac{k^2 - q^2}{k^2 + q^2} \right] \quad (3.1)$$

and

$$k > q, \varphi_s = \pi \quad r_s = \frac{1}{2} \left[ -\frac{C_R}{U_T} \frac{q^2}{q^2 + k^2} \pm D^{1/2} \right] \quad (3.2)$$

We note that the values for  $r_s$  in (3.1) and (3.2) are obtained from quadratic equations, but that only one sign can be retained in the square root because  $r_s$  shall be positive.

Turning next to the case where  $k < q$  we notice that a possibility is again  $\varphi_s = 0$  in which case we obtain:

$$k < q, \quad \varphi_s = 0 \quad r_{s1,2} = \frac{1}{2} \left[ \frac{C_R}{U_T} \frac{q^2}{q^2 + k^2} \pm D^{1/2} \right]. \quad (3.3)$$

It is, however, seen from (3.3) that these steady states exist only when the radicand is positive. This requirement leads to the condition that  $U_T$  is restricted to values satisfying the inequality

$$U_T < \frac{1}{2} C_R \frac{q^2}{(q^4 - k^4)^{1/2}}. \quad (3.4)$$

These two steady states, both characterized by a non-sloping structure, exist only when  $U_T$  is sufficiently small.

One must investigate the possibility of  $\varphi_s = \pi$  also in the case of  $k < q$ . However, in that case the value of  $r_s$  would be computed from

$$r_s = \frac{1}{2} \left[ -\frac{C_R}{U_T} \frac{q^2}{q^2 + k^2} + D^{1/2} \right] \quad (3.5)$$

and it is seen from (3.5) that  $r_s > 0$  cannot be satisfied.

The last possibility to satisfy (2.10) when  $\varphi_s$  is different from 0 and  $\pi$  is to have

$$k < q \quad r_s = \left( \frac{q^2 - k^2}{q^2 + k^2} \right)^{1/2} \quad (3.6)$$

in which case we obtain from (2.7) that

$$\cos \varphi_s = \frac{1}{2} \frac{C_R}{U_T} \frac{q^2}{(q^4 - k^4)^{1/2}}. \quad (3.7)$$

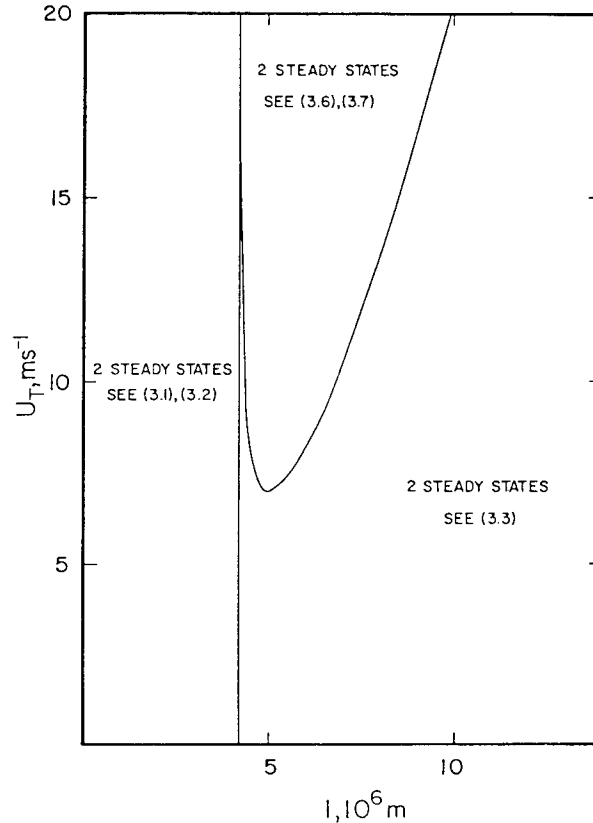


Fig. 1. A summary of the regions in which the various steady states exist including references to the appropriate equations.

Since  $\cos\varphi_s < 1$  we can use (3.6) only when

$$U_T > \frac{1}{2}C_R \frac{q^2}{(q^4 - k^4)^{1/2}}. \quad (3.8)$$

When (3.7) is satisfied we obtain two values,  $\varphi_s$  and  $-\varphi_s$ , from (3.7) each for the same value of  $r_s$  as given in (3.6).

The existence of the various steady states are shown in Fig. 1. We obtain a total of six steady states, two in each of the three regions of the diagram where the curve corresponds to an equality sign in (3.4) or (3.8).

It should not go unnoticed that the curve and the asymptote in Fig. 1 is identical to the critical curve in the stability problem using the two-level, quasi-nondivergent model. In our case, the curve represents the division of a region with sloping steady state and one with a non-sloping vertical structure. In the stability study the curve separates a region of instability from another region of stability. It is not surprising that the same curve should appear in both problems because a distinguishing factor in the stability problem is that the amplifying waves tilt westwards enabling them to transport heat from south to north.

#### 4. The stability of the steady states

The stability of the six steady states is investigated using a linearized version of the equations (2.7) and (2.10). If  $(r_s, \varphi_s)$  is an arbitrary steady state, and  $(r', \varphi')$  a small deviation from the steady state, we can derive the linear perturbation equations. They are:

$$\begin{aligned} \frac{dr'}{dt} &= -kU_T [2r_s \sin\varphi_s r' + (r_s^2 + \frac{k^2 - q^2}{k^2 + q^2}) \cos\varphi_s \cdot \varphi'] \\ \frac{d\varphi'}{dt} &= kU_T [(1 + \frac{k^2 - q^2}{k^2 + q^2} \frac{1}{r_s^2}) \cos\varphi_s r' - r_s (1 - \frac{k^2 - q^2}{k^2 + q^2} \frac{1}{r_s^2}) \sin\varphi_s \cdot \varphi']. \end{aligned} \quad (4.1)$$

In obtaining the system (4.1), it has been assumed that  $\cos\varphi' = 1$  and  $\sin\varphi' = \varphi'$ . We can easily investigate the stability of the first four steady states because they are characterized by having  $\varphi_s = 0$  or  $\varphi_s = \pi$ . In both cases (4.1) reduces to the following equations:

$$\begin{aligned} \frac{dr'}{dt} &= -kU_T (r_s^2 + \frac{k^2 - q^2}{k^2 + q^2}) \cos\varphi_s \varphi' \\ \frac{d\varphi'}{dt} &= kU_T \frac{1}{r_s^2} (r_s^2 + \frac{k^2 - q^2}{k^2 + q^2}) \cos\varphi_s r' \end{aligned} \quad (4.2)$$

where  $\cos\phi_s = 1$ , or  $-1$ .

We look for solutions of the form  $(r', \varphi') = (r'_0, \varphi'_0) \exp(\nu t)$  and find from (4.2) that

$$\nu^2 + (kU_T)^2 \frac{1}{r_s^2} \left( r_s^2 + \frac{k^2 - q^2}{k^2 + q^2} \right)^2 \cos^2 \varphi_s = 0 \quad (4.3)$$

It is obvious from (4.3) that  $\sigma$  is a purely imaginary number regardless of whether  $\cos \varphi_s = 1$  or  $\cos \varphi_s = -1$ . The frequency is

$$\nu = \pm i(kU_T) \frac{1}{r_s} \left( r_s^2 + \frac{k^2 - q^2}{k^2 + q^2} \right)^{1/2} \quad (4.4)$$

where  $r_s$  is obtained from (3.2) or (3.3). We conclude therefore that the four steady states having  $\varphi_s = 0$  or  $\varphi_s = \pi$  are stable. Deviations from a steady states will in these cases result in oscillations around the steady state.

We proceed next to the steady states for  $k < q$  described by (3.6), (3.7) and (3.8). Since

$$r_s^2 = \frac{q^2 - k^2}{q^2 + k^2} \quad (4.5)$$

in this case, we find that

$$\begin{aligned} \frac{dr'}{dt} &= -2kU_T \sin \varphi_s r' \\ \frac{d\varphi'}{dt} &= -2kU_T \sin \varphi_s \phi' \end{aligned} \quad (4.6)$$

or

$$\nu = -2kU_T \sin \varphi_s \quad (4.7)$$

Assuming that  $U_T > 0$  as it is in the troposphere we conclude from (4.7) that the steady state having  $0 < \varphi_s < \pi$  is stable ( $\nu_r < 0$ ) while the other steady state with  $-\pi < \varphi_s < 0$ , is unstable ( $\nu_r > 0$ ).

We have thus shown that of the six steady states only one is unstable for  $U_T > 0$ . Of the remaining five steady states one represents a wave for which  $\varphi = \theta_* - \theta_T > 0$  meaning that the temperature field is lagging behind the geopotential field, or, equivalently, a westward slope with height. It is this stable steady state which is the asymptotic state of the amplifying baroclinic wave created by the growth of infinitesimal disturbances on an unstable zonal current. The remaining four stable, steady states have no slope in the vertical direction. In the cases where  $\varphi_s = 0$ , we have obviously a geopotential wave of the form

$$\phi_* = \hat{\phi}_* \cos kx, \quad \phi_T = \hat{\phi}_r \cos kx \quad (4.8)$$

resulting in

$$\phi_1 = (\hat{\phi}_* + \hat{\phi}_T) \cos kx, \quad \phi_3 = (\hat{\phi}_* - \hat{\phi}_T) \cos kx \quad (4.9)$$

In the other case where  $\varphi_s = \pi$ , we have

$$\phi_* = \hat{\phi}_* \cos kx, \quad \phi_T = \hat{\phi}_T \cos(kx + \pi) \quad (4.10)$$

which results in a wave with no slope, but with a decreasing amplitude with height because

$$\phi_1 = (\hat{\phi}_* - \hat{\phi}_T) \cos kx, \quad \phi_3 = (\hat{\phi}_* + \hat{\phi}_T) \cos kx \quad (4.11)$$

These four steady states correspond therefore to waves with an equivalent barotropic structure.

It is of interest to look at the relative structure of the various wave types. All calculations are carried out with parameters for  $45^\circ\text{N}$ . Fig. 2 shows  $r_s$  as a function of wave length for the cases  $\varphi_s = 0$  and  $\varphi_s = \pi$  up to a wave length corresponding to  $k = q$  or  $L_* = 2\pi/q \approx 4.2 \times 10^6 \text{m} = 4200 \text{km}$ .  $U_T = 5 \text{m}^{-1}$  has been used. For small values of  $L$  we find  $r_s$  close to unity, while the wave with  $\varphi_s = 0$  approaches the value 0.7 as  $k$  approaches  $q$ . We may verify this result from (3.1) which for  $k = q$  gives

$$r_s = \frac{1}{2} \frac{\beta}{U_T q^2} = 0.72$$

For the case  $\varphi_s = \pi$  we find from (3.2) that  $r_s$  is zero as can also be seen from Fig. 2.

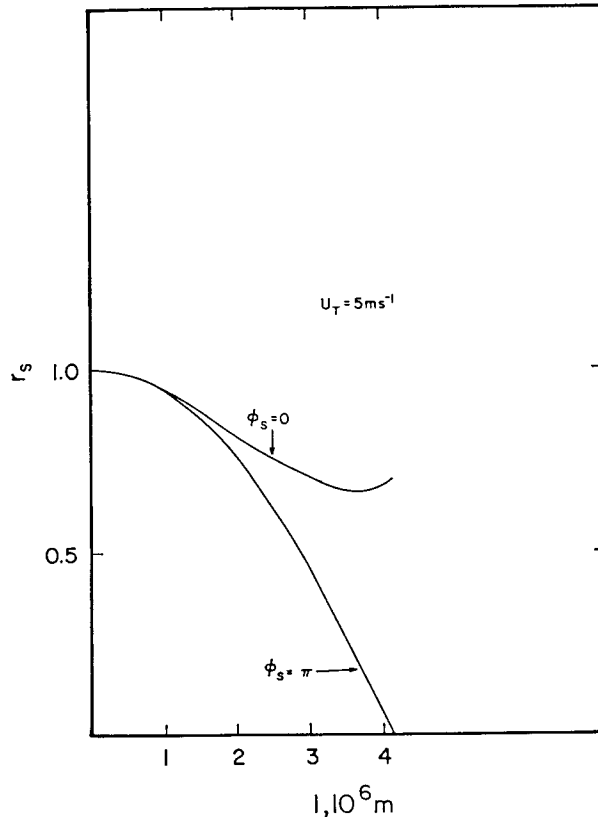


Fig. 2. The relative amplitude as a function of wavelength for the short waves ( $L < 2\pi/q$ ) for the cases of the phase angle being 0 and  $\pi$ .  $U_T = 5 \text{m s}^{-1}$ .



Fig. 3 shows for the same value of  $U_T = 5 \text{ m s}^{-1}$  the two amplitudes for  $\varphi_s = 0$ . The value corresponding to the minus sign in (3.3) remains small for increasing values of the wavelength indicating

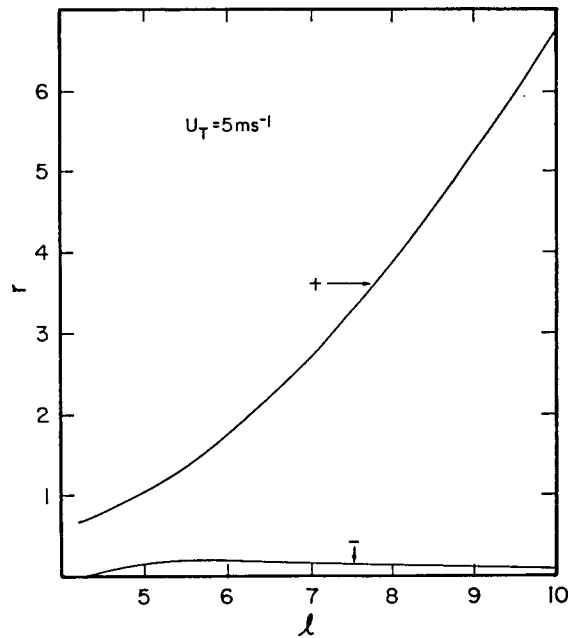


Fig. 3. The relative amplitudes as a function of wavelength for long waves ( $L/2$ ) with subcritical windshear ( $U_T = 5 \text{ m s}^{-1}$ ) and phase angle  $\varphi_s = 0$ .

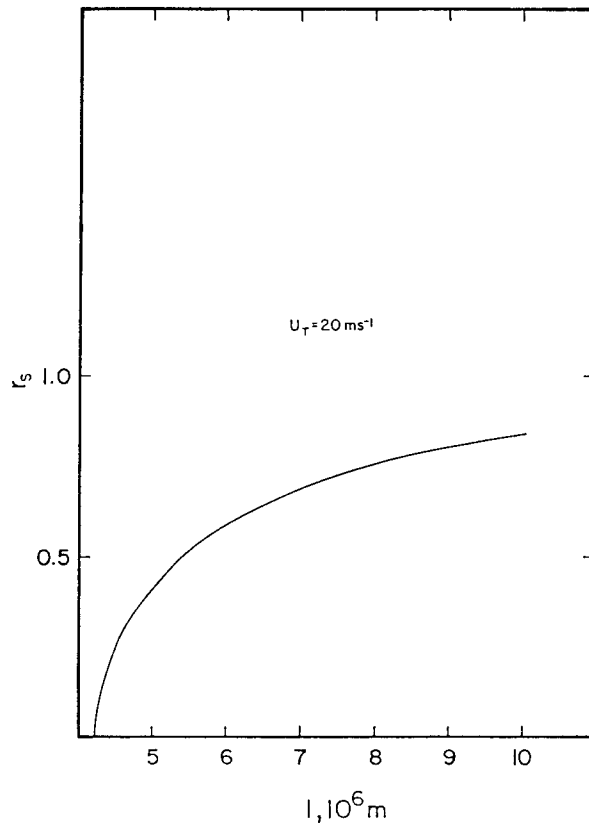


Fig. 4. The relative amplitude as a function of wavelength for long waves ( $L > 2\pi/q$ ) with supercritical windshear ( $U_T = 20 \text{ m s}^{-1}$ ).

that the amplitudes at the upper and the lower levels are of the same order of magnitude. On the other hand, corresponding to plus sign in (3.3)  $r_s$  increases with increasing wavelength and attains values larger than unity when  $L > 5000$  km corresponding to a phase difference of  $\pi$  between the geopotential at the upper and lower levels.

Fig. 4 depicts  $r_s$  as a function of wave length for  $U = 20 \text{ m s}^{-1}$  and  $\varphi_s > 0$ .  $r_s < 1$  for all wavelength. The phase difference  $\varphi_s > 0$  is shown in Fig. 5 as a function of wavelength for the same case.

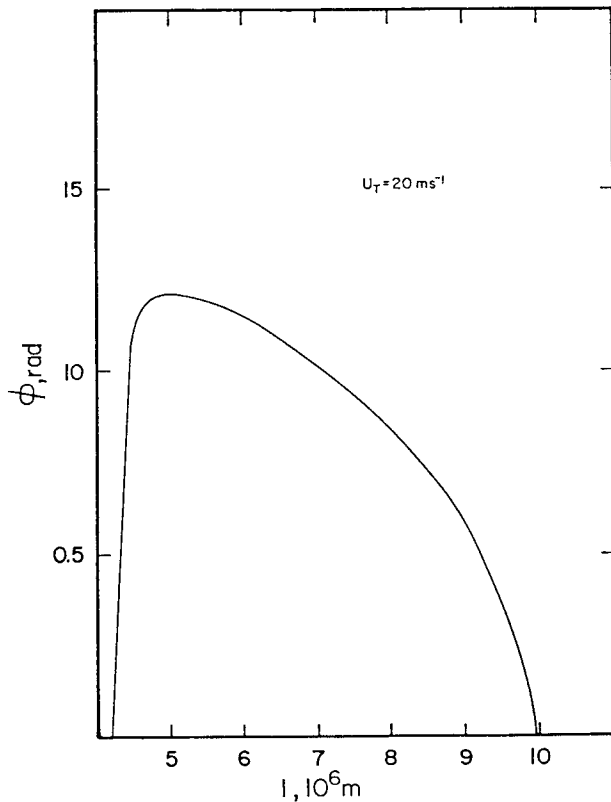


Fig. 5. The phase angle  $\varphi_s = \theta_s - \theta_T$  as a function of wavelength for the same case as in Fig. 5.

We show finally a few time integrations of the nonlinear equations (2.7) and (2.10). Fig. 6 shows the stable oscillation of  $r$  and  $\varphi$  for a case where  $U_T = 20 \text{ m s}^{-1}$  and  $L = 2000$  km starting from a state of  $r = 0.8$  and  $\varphi = 0.05$ . The period is 1.46 days. Fig. 7 gives the oscillation in  $\varphi$  for a case of  $U_T = 4 \text{ m s}^{-1}$  and  $L = 5000$  km. The period is very close to 11.88 days.

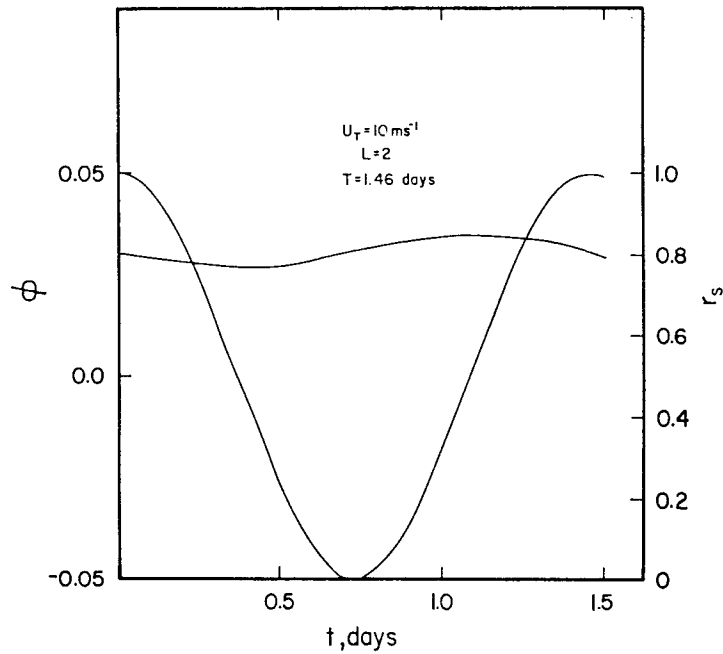


Fig. 6. The curves  $\varphi(t)$ ,  $r(t)$  for a time integration of the nonlinear equations.  $U_T = 10 \text{ m s}^{-1}$ ,  $L = 2000 \text{ km}$ , period = 1.46 days.  $\varphi$  -scale on the left and  $r$  -scale on the right side.

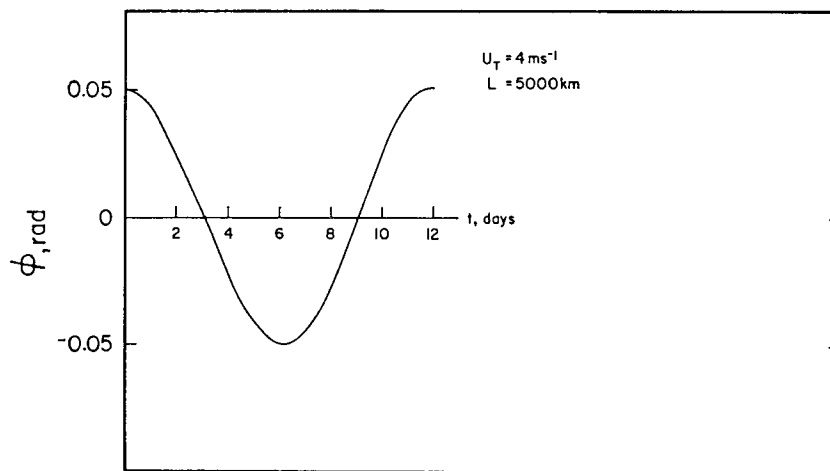


Fig. 7. Same arrangement as in Fig. 6 but, for a case with  $U_T = 4 \text{ m s}^{-1}$ ,  $L = 5000 \text{ km}$ . The period is a little less than 12 days.

The remaining case refers to the waves with a significant vertical slope. A case with  $U_T = 8 \text{ m}^{-1}$  and  $L = 5000 \text{ km}$  was selected. It has steady states with  $r_s = 0.4186$  and  $\varphi_s = \pm 0.5$ . Fig. 8 shows  $\varphi = \varphi(t)$  for an initial state of  $r_0 = 0.4186$  and  $\varphi_0 = -0.45$ , i.e., close to the unstable steady state. The curve shows that  $\varphi$  approaches the phase angle  $\varphi_s = 0.5$  after an integration over more than 20 days. The variation of  $r = r(t)$  is almost insignificant in this case. On the other hand, if one starts on the other side of the unstable steady state, say  $r_0 = 0.4186$  and  $\varphi_0 = -0.55$ , we find again by an integration of the equations that solutions after approximately 20 days is close to the stable steady state as shown by the curve  $\varphi = \varphi(t)$  in Fig. 9.

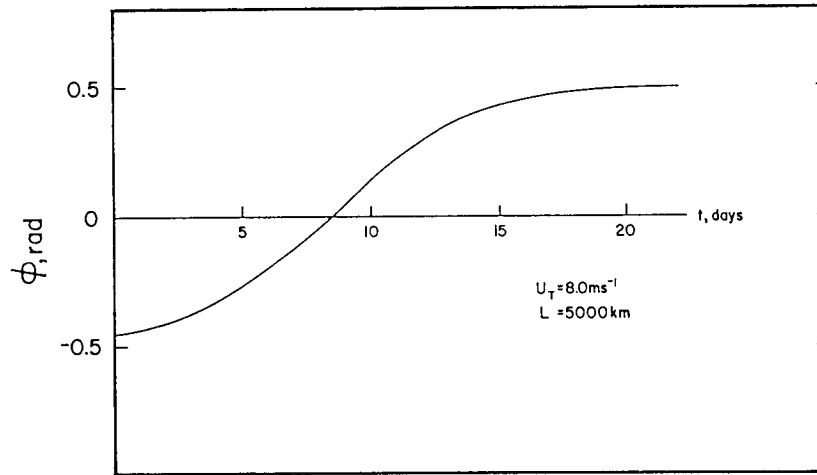


Fig. 8. The phase angle  $\varphi$  as a function of time for the case  $r_0 = 0.4186$ ,  $\varphi_0 = -0.45$ ,  $U_T = 8 \text{ m s}^{-1}$ ,  $L = 5000 \text{ km}$ . The unstable steady state has  $\varphi_s = -0.05$ , while the stable steady state has  $\varphi_s = 0.05$ .

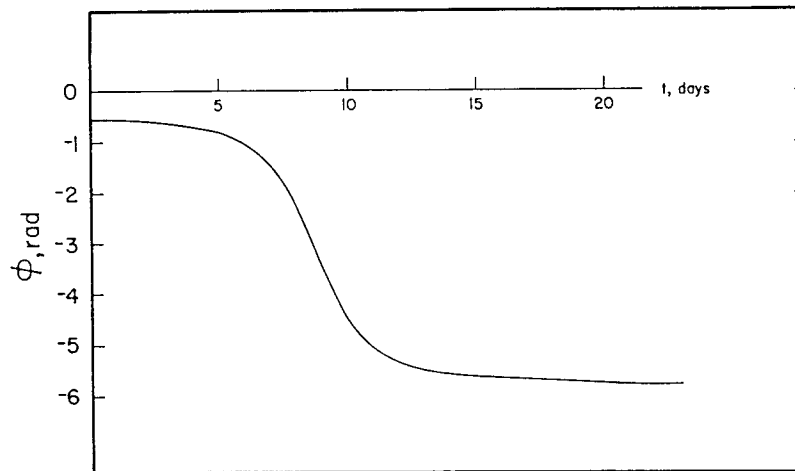


Fig. 9. As Fig. 8, but with starting values of  $r_0 = 0.4186$  and  $\varphi_0 = -0.55$ . The asymptotic value is  $\varphi = -5.78$  corresponding  $-5.78 + 2\pi = 0.5$ .

### Conclusions

The main conclusion from this study is that there exists a stable steady state with a westward slope with height in the region for which a zonal flow with a sufficiently large thermal wind is unstable. A steady state with the opposite slope is unstable. This result gives a natural explanation for the observed structure of the transient waves in the atmosphere as described by data studies. For the sake of completeness, we have also found the steady states in the other parts of the  $(L, U_T)$  diagram. They are stable, but will in general have either a slope of half a wavelength or no slope at all, but the significance of the latter results is smaller because no mechanism in the model will create these disturbances.

The approach to the problem has deliberately been held in the most simple terms employing not only the two level, quasi-nondivergent model, but also very simple zonal currents and waves. The study could in all likelihood be expanded to become more general. One could, for example, consider waves on a zonal current with horizontal as well as vertical wind shear and thus consider a mixed barotropic-baroclinic problem. Heating and dissipation could be added to the present study without difficulty. It may also be possible to consider a model with a continuous variation in the vertical direction of both the zonal current and the waves.

### REFERENCES

- Charney, J. G., 1947. The dynamics of long waves in a baroclinic westerly current, *J. of Meteor.* **4**, 135-162.
- Ogura, Y., 1957. Wave solution of the vorticity equation for the 2-1/2-dimensional model. *J. of Meteor.*, **14**, 60-64.
- Palmén, E. and C. Newton, 1969. Atmospheric circulation systems. Academic Press, New York.
- Thompson, P. D., 1959. Some statistical aspects of the dynamic processes of growth and occlusion in simple baroclinic models, Rossby Memorial Volume, Rockefeller Institute Press, 350-358.
- Wiin-Nielsen, A., 1961. A note on the behavior of very long waves in simple baroclinic models, *J. of Meteor.*, **18**, 204-207.
- Wiin-Nielsen, A., 1973. Dynamic Meteorology, World Meteorological Organization, No. 364.